Thomson-Scattering Study of the Subharmonic Decay of Ion-Acoustic Waves Driven by the Brillouin Instability

H. C. Bandulet,[1] C. Labaune,[1] K. Lewis,[1,2] and S. Depierreux[2]

[1]*Laboratoire pour l'Utilisation des Lasers Intenses, UMR 7605 CNRS-Ecole Polytechnique-CEA-Université Paris Virgin Islands, Ecole Polytechnique 91128 Palaiseau Cedex, France*

[2]*CEA-DIF, BP 12, 91680 Bruyères-Le-Châtel, France*

(Received 3 November 2003; published 13 July 2004)

Thomson scattering (TS) has been used to investigate the two-ion decay instability of ion acoustic waves generated by stimulated Brillouin scattering in an underdense CH plasma. Two complementary TS diagnostics, spectrally and spatially resolved, demonstrate the occurrence of the subharmonic decay of the primary ion acoustic wave into two secondary waves. The study of the laser intensity dependence shows that the secondary ion acoustic waves are correlated with the SBS reflectivity saturation, at a level of a few percent.

DOI: 10.1103/PhysRevLett.93.035002 PACS numbers: 52.35.Fp, 52.25.Os, 52.38.–r, 52.50.Jm

The propagation of an intense laser beam within a long scale-length underdense plasma can give rise to parametric instabilities such as the stimulated Brillouin scattering instability (SBS) [1]. It consists in the decay of the incident electromagnetic wave into an ion acoustic wave (IAW) and a scattered electromagnetic wave. SBS represents a serious threat to inertial confinement fusion schemes as it may cause the reflection of a large fraction of laser energy and spoil the uniformity of the irradiation. Experiments carried out in the context of fusion [2] have reported limited levels of backscattering, less than 30%, which are much lower than the levels predicted by most theoretical models, which in some cases reach 100%. Nevertheless, such high levels have been measured under certain conditions [3]. The physical mechanisms responsible for the limited SBS reflectivity and for its saturation are not yet clear. Pump depletion in the highest intensity regions of the focal volume could be partly responsible. In these areas of active SBS, the nonlinearity of the plasma response gives way to a variety of phenomena that could also reduce the SBS growth, including ion tail formation, ion trapping, high-harmonics generation, and nonlinear frequency shifts (see Ref. [4], and references therein). Among the different processes, the decay of the SBS (primary) IAW into two secondary IAW has been proposed as a mechanism to limit the amplitude of the primary IAW. This instability, referred to as the *two-ion decay* (TID) instability, has been predicted in several theoretical and numerical studies [5,6].

In this Letter, we present the first observation, using Thomson scattering, of such secondary IAW and of their correlation with the primary SBS-driven IAW in time and space, as well as the evolution of their relative amplitudes with the laser intensity. An important result is that the secondary IAW were only observed in the range of intensities where the SBS reflectivity was in the saturated regime. This could be evidence of their participation in the saturation of SBS. The amplitudes of the primary and secondary waves, which were collected using separate optics, have been measured. At a laser intensity of $\sim 1.0 \times 10^{16}$ W/cm^2, the ratio between the primary and secondary waves was close to ~8–10 with the assumption of a coherent emission—an indication that the secondary waves are not negligible.

The experiments were carried out using five of the six ~600-ps FWHM lasers beams of the nanosecond facility at the Laboratoire pour l'Utilisation des Lasers Intenses (LULI). All beams were in the horizontal plane. The plasma was created from a 1.2-μm-thick, 380-μm-wide CH ($\langle Z \rangle = 3.5$) foil irradiated by two $\lambda = 0.53$ μm counterpropagating beams. The plasma was then heated by a third identical beam with a delay of 0.6 ns. Random-phase plates (RPP) were used on the creation and heating beams for plasma reproducibility. The plasma's main expansion axis (z axis) was perpendicular to the target's initial surface ($z = 0$). The plasma was well characterized in previous experiments [7]. Its maximum density at the peak of the interaction pulse, which was $n_{\max} \sim 0.15 n_c$ (where $n_c = 1 \times 10^{21}$ cm^{-3} is the critical density for 1.053 μm light), decreased exponentially in time as $n_{\max}(t) = n_{\max} \exp(-t[\text{ps}]/530)$. The typical scale length of the plasma's inverse parabolic profile was ~700 μm. The measured electron temperature was between 500–700 eV and ion temperature was estimated at ~200 eV, so that $ZT_e/T_i \sim 9$. With a 1.7 ns delay after the heating beams, a 1.053-μm interaction beam focused by a $f = 50$ cm lens was sent propagating along the z axis (towards $z > 0$). In the following, we will refer to the front part of the plasma as the entrance side of the interaction beam with $z < 0$. The beam diameter was reduced to 50 mm with the use of a diaphragm, which selected a quasi–plane wave front in the laser beam, in order to produce a focal spot close to the limit of diffraction. The 2D far-field images of the intensity distribution showed that 50% of the laser energy was contained

within a spot of 15 μm in diameter leading to a maximum intensity of 1.0×10^{16} W/cm^2.

An $f/3$, $\lambda_p = 0.35$ μm, low-intensity ($\langle I \rangle \sim 4 \times 10^{12}$ W/cm^2) probe beam was used for Thomson scattering (TS) off the IAW. It was synchronized with the interaction beam and sent at 67.5° from the interaction beam axis. The TS light was collected by a $f/1.5$ off-axis parabola and sent to two different stations: (i) a 1D time-resolved imaging system of the plasma spatially resolved along the z axis with a 100 ps temporal resolution and (ii) a spectrometer coupled to a multislit S1 streak camera enabling simultaneous observation of the time-resolved spectra of the TS light at different locations along the z axis. The spectral and temporal resolutions were, at best, 0.8 Å and 160 ps. The parabola was centered at 81° from the z axis and had an effective aperture of 34°. Masks were placed on the probe beam (reducing its effective aperture to $f/8$) and the collection optics to select the wave-vector magnitude and direction of the probed IAW.

The two instabilities considered in this experiment are shown schematically in Fig. 1. In the SBS instability [see Fig. 1(a)], the incoming electromagnetic (EM) wave ($\mathbf{k}_0$, ω_0) parametrically decays into an ion wave ($\mathbf{k}_{iaw}$, ω_{iaw}) and a backscattered EM wave ($\mathbf{k}_{SBS}$, ω_{SBS}). The TID instability [see Fig. 1(b)], consists in the decay of the SBS-driven ion wave into two secondary IAW ($\mathbf{k}_{iaw}^{1,2}$, $\omega_{iaw}^{1,2}$) directed at a variable angle η. The geometry of the experiment [see Fig. 1(c)] was designed, using the matching conditions and the linear dispersion relations of the IAW, to collect the down-Thomson scattered light off primary IAW associated with near-backward SBS ($\varepsilon < 25°$) and secondary IAW associated with the decay of the primary waves at angles η between 0 and 20° from the primary waves. Figure 1(d) shows the calculated scattering angle δ as a function of the probe angle θ for the primary IAW and for four of its decay products (see Ref. [8] for more details). The diagram has been limited to the accessible angles in the experiment. To study the primary IAW driven by SBS, the probe beam angles θ and collection angles δ were chosen, respectively, between [66,5° 73,5°] and between [72° 77°] from the interaction beam axis (window 1). The scattered light off secondary IAW was collected between angles $\delta \in [90° 95°]$ using two probe beam apertures: $\theta \in [66{,}5° 73{,}5°]$ (window 2) and $\theta \in [73° 78°]$ (window 3). The probe beam and collection apertures of window 2 were optimized for the observation of IAW that satisfy the conditions $k_{iaw}^{1,2} \approx k_{iaw}/2$ and $\omega_{iaw}^{1,2} \approx \omega_{iaw}/2$, for which simulations predict the maximum growth rate [6] of $\approx (\partial N/N)\omega_{iaw}/4$. Window 3 was selected to detect the decay modes, $k_{iaw}/3$ and $k_{iaw}/4$. In our conditions, the product of the wave vector by the Debye length is $k_{iaw}\lambda_D \sim 0.15$ for the primary IAW. Wave vector magnitudes ranging from $1.5k_0$ to $2.1k_0$ (k_0 in vacuum) for the primary waves, from $0.6k_0$ to $1.2k_0$ for the secondary waves in window 2, and from $0.4k_0$ to $0.9k_0$ for window 3 could be detected by the diagnostic. The solid angles of the probe beam and of the collection optics were the same for windows 1 and 2, providing a relevant comparison of the Thomson scattered intensities.

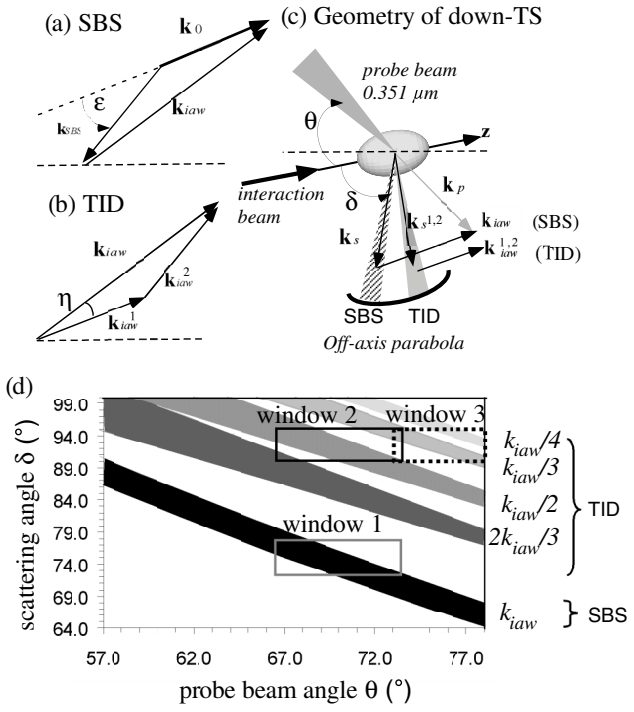

FIG. 1. Vector-diagram of (a) the backward SBS geometry and (b) the TID geometry: the primary wave ($\mathbf{k}_{iaw}$, ω_{iaw}) decays into two secondary IAW ($\mathbf{k}_{iaw}^{1,2}$, $\omega_{iaw}^{1,2}$) propagating at a small angle η. (c) Experimental setup and wave-vector diagram for down-TS off the primary and secondary IAW. This latter satisfies $\mathbf{k}_s = \mathbf{k}_p - \mathbf{k}_{iaw}$ and $\omega_s = \omega_p - \omega_{iaw}$. (d) Scattering angle δ as a function of the probe beam angle θ, both measured from the z axis, that satisfy the matching conditions for the primary IAW and four of its decay products.

A complementary diagnostic was set up to study the backscattered EM waves associated with SBS. The scattered light, collected within the laser-focusing aperture, was analyzed in spectrum (using a spectrometer-streak combination) and in energy (using a fast photodiode). The collected light included pure backscattering and side scattering up to an angle of 5° from the laser axis. The reflectivity dependence on the laser intensity, shown in Fig. 2, consists of an exponential growth, between intensities 10^{13} and 10^{15} W/cm^2, followed by saturation at a near constant level of ~5–10% for laser intensities greater than 10^{15} W/cm^2. The SBS spectra are wide and completely blueshifted.

Two examples of TS spectra off IAW associated with SBS and TID, using the three combinations of masks, are shown in Fig. 3 for a laser intensity of 5×10^{15} W/cm^2. The diagnostic collected light emitted from a plasma slab of a height of 50 μm in the case of the primary waves and

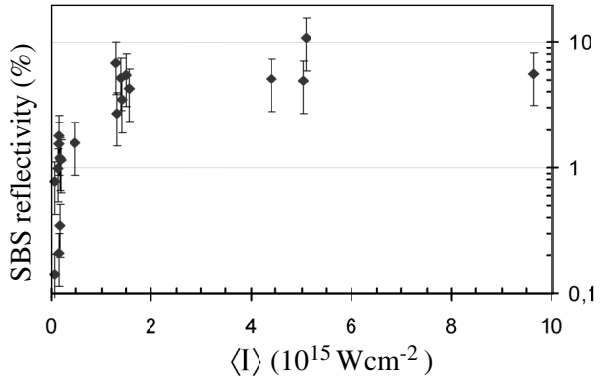

FIG. 2. Time-integrated average SBS reflectivity as a function of the average intensity of the $f/10$ interaction beam.

of 150 μm in the case of the secondary waves. The slab was 25 μm in width and was located at $z = -350$ μm. This location corresponded to maximum SBS activity according to both the TS imagery diagnostic and the backward SBS diagnostic. In the latter case, the spectral shift of the backscattered light agreed with the net blueshift due to the Doppler effect of the expanding plasma around -350 μm [9].

The blueshifts of the three TS spectra are in agreement with the calculated values: $d\omega = \omega_{iaw} = k_{iaw}[c_s - u(z)]$, where c_s is the sound velocity and $u(z)$ is the plasma flow velocity (deduced from thermal TS measurements). Assuming an expansion velocity of $u(-350\ \mu\text{m}) \sim 3.0 \times 10^7$ cm/s and k_{iaw} between $1.5k_0$ and $2.1k_0$ this formula predicts blueshifts between (0.8–1.2) Å for the scattered light off the primary waves collected in window 1. In the case of the scattered light off $k_{iaw}/2$ secondary waves, the mean shift is expected to be between (0.4–0.6) Å. The spectral shift of the light collected in window 3 should be about 0.3 Å, as observed in Fig. 3(b). In order to detect the scattering off the secondary waves in windows 2 and 3, a larger spectrometer slit was used to collect a significant signal, which lowered the spectral resolution to 2 Å.

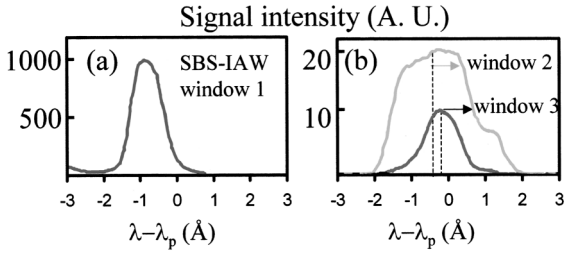

FIG. 3. Spectra of IAW at $z = -350$ μm in the front part of the plasma collected (a) in window 1, (b) in window 2 (gray solid line) and in window 3 (black solid line). The spectra have been time-integrated over 200 ps. Intensity scale is relative and given in arbitrary units. The spectral resolutions for the primary IAW [(a)] and secondary IAW [(b)] are 0.8 and 2.0 Å, respectively.

The signal collected in window 2 was on the average 50–100× weaker than the signal associated with SBS-IAW and stronger by a factor of 2 than that collected in window 3. This demonstrates that the $k_{iaw}/2$ decay mode has a greater growth rate than either the $k_{iaw}/3$ or $k_{iaw}/4$, as suggested by the numerical results. This diagnostic already provides a clear identification of IAW produced by the decay of the primary SBS IAW. Such waves have also been detected in a gold (Au) plasma, but presented a broad k spectrum [10].

More complete information about the spatial evolution of the amplitude of the two types of IAW within the density profile along the z axis was obtained from the imaging diagnostic which was also temporally resolved. This diagnostic collected light emitted from a 75-μm-high plasma slab over the spectral range of (3510 ± 10) Å. Figure 4 displays two frames showing the Thomson scattered light intensity off IAW associated with backward SBS [Fig. 4(top)] and with TID [Fig. 4(middle)] as a function of space (z) and time. The SBS-IAW signal was a hundred times more attenuated than the TID-IAW signal. The most interesting result is the complete correlation in space and time of the two types of IAW. They both grow in the front part of the plasma, with a maximum around 350 μm from the initial target plane, and occur during the first half of the laser pulse. This result has already been obtained, with an RPP

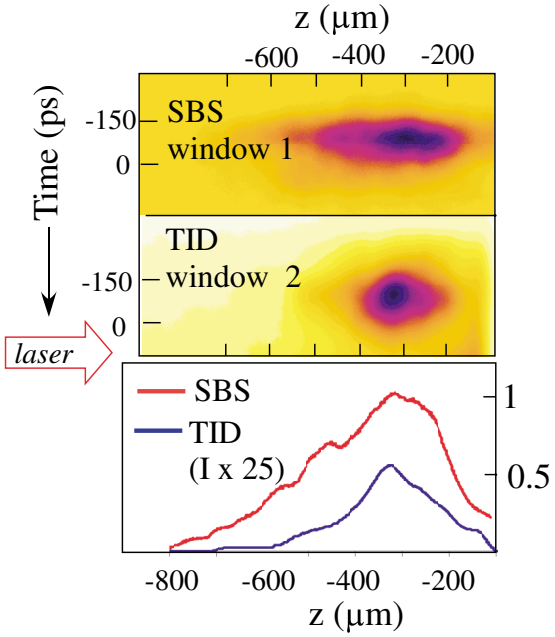

FIG. 4 (color online). Time-resolved intensity image along the z axis of IAW associated with SBS collected in window 1 (top) and of IAW collected in window 2 associated with TID (middle). Bottom: lineouts in Z of the SBS (red/upper curve) and TID (blue/lower curve) images averaged over 100 ps and given in relative signal intensity. The TID signal in the lineout has been multiplied by 25.

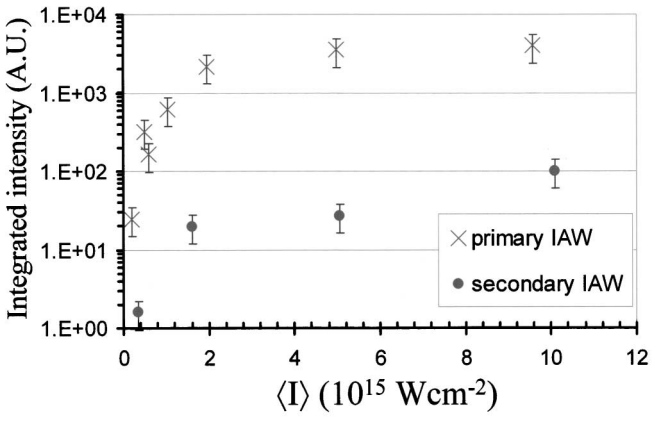

FIG. 5. Time-integrated Thomson scattered signal off primary IAW associated with SBS (collected in window 1) and secondary IAW (collected in window 2) at $z = -350$ μm in the front part of the plasma as a function of the average laser intensity.

irradiation, for the IAW associated with SBS [9]. The novelty is the evidence of IAW that present the spatial, temporal, and spectral properties of the subharmonics produced by the TID instability of the SBS-driven IAW.

Once the waves were well identified, we proceeded to the relative measurements of the scattered intensity off the IAW associated with SBS collected in window 1 with the secondary IAW collected in window 2 as a function of the laser intensity. The results are plotted in Fig. 5. The points are time-integrated scattered signals at $z = -350$ μm. For laser intensities lower than 9×10^{14} W/cm^2, the TS light off TID-IAW was below the detection threshold. Above this value, there is a fast increase of the TID-IAW scattered light. The dots for SBS-IAW are consistent with the SBS reflectivities of Fig. 2. The secondary IAW were detected only at laser intensities for which the SBS reflectivity was in a saturated regime. In fact, there was no evidence of TS light from TID-IAW when a RPP was added to the interaction beam, the intensity of which thus reduces to 8×10^{13} W/cm^2 in a focal spot diameter of 320 μm. The SBS reflectivity curve for this type of irradiation was measured in a previous experiment and did not show saturation [see Figure 6(c) of Ref. [7]]. Although high-intensity speckles account for most of the SBS, which is likely in a saturated regime, the level of secondary IAW in the probed volume was probably too small to be detected. Assuming that the scattering comes from a coherent IAW, the Thomson scattered power (P_s) is proportional to the square of the density fluctuation level $(\delta n/n)^2$ associated with the IAW [11]. With the values computed in Fig. 5, we estimate the IAW amplitude ratio between the secondary and primary IAW to be of approximately 8–10 for a laser intensity close to 10^{16} W/cm^2.

In summary, IAW associated with the TID instability of SBS-driven ion waves were observed using two independent Thomson scattering diagnostics. The Thomson spectra enabled unambiguous identification of the waves and the spatial imaging diagnostic allowed us to establish a good correlation between the primary and the secondary IAW. Although the complete spectrum of IAW could not be probed in this experiment, the fact that the secondary waves associated with the TID instability were only observed when the SBS reflectivity was in the saturated regime is a strong indication that TID plays a role in the saturation of SBS, alongside other possible participating mechanisms.

We gratefully acknowledge the support of A. Michard and the LULI staff during the experiments. We would also like to thank C. Riconda, D. Pesme, S. Hüller, F. Detering, S. Glenzer, and E. A. Williams for valuable discussion. Part of this work was supported by the Ministry of Natural Ressources of Quebec.

[1] W. Kruer, *The Physics of Laser-Plasma Interactions* (Addison-Wesley, New York, 1988).
[2] L. V. Powers *et al.*, Phys. Plasmas **2**, 2473 (1995); B. J. MacGowan *et al.*, *ibid.* **3**, 2029 (1996); R. P. Drake, R. G. Watt, and K. Estabrook, Phys. Rev. Lett. **77**, 79 (1996); J. C. Fernandez *et al.*, *ibid.* **81**, 2252 (1998); S. P. Regan *et al.*, Phys. Plasmas **6**, 2072 (1999); J. D. Moody *et al.*, Phys. Rev. Lett. **86**, 2810 (2001).
[3] J. Handke, S. A. H. Rizvi, and B. Kronast, Appl. Phys. **25**, 109 (1981).
[4] L. Divol *et al.*, Phys. Plasmas **10**, 3728 (2003).
[5] J. Kartunnen *et al.*, Phys. Fluids **24**, 447 (1981); J. A. Heikkinen, S. J. Kartunnen, and R. R. E. Salomaa, Phys. Fluids **27**, 707 (1984); C. Riconda *et al.*, Phys. Scr. **T84**, 217 (2000).
[6] B. I. Cohen *et al.*, Phys. Plasmas **4**, 956 (1997).
[7] J. Fuchs *et al.*, Phys. Plasmas **7**, 4659 (2000).
[8] H. C. Bandulet *et al.*, *Rapport Annuel du Laboratoire pour l'Utilisation des Lasers Intenses, Palaiseau*, 2002.
[9] C. Labaune *et al.*, Phys. Rev. Lett. **76**, 3727 (1996).
[10] C. Niemann *et al.*, Bull. Am. Phys. Soc. **45**, UP1.032 (2003).
[11] J. Sheffield, *Plasma Scattering of Electromagnetic Radiation* (Academic Press, London, 1975).